# We are IntechOpen, the world's leading publisher of Open Access books Built by scientists, for scientists

## 6,900
Open access books available

## 185,000
International authors and editors

## 200M
Downloads

## 154
Countries delivered to

Our authors are among the

## TOP 1%
most cited scientists

## 12.2%
Contributors from top 500 universities

**CLARIVATE ANALYTICS**
**BOOK CITATION INDEX**
**INDEXED**

**WEB OF SCIENCE**™

Selection of our books indexed in the Book Citation Index
in Web of Science™ Core Collection (BKCI)

## Interested in publishing with us?
## Contact book.department@intechopen.com

# Simulations Suggest Possible Triply Bonded Phosphorus≡E13 Molecules (E13 = B, Al, Ga, In, and Tl)

Jia-Syun Lu, Ming-Chung Yang and Ming-Der Su

Additional information is available at the end of the chapter

**Abstract**

The effect of substitution on the potential energy surfaces of RE13 ≡ PR (E13 = B, Al, Ga, In, Tl; R = F, OH, H, CH3, SiH3, SiMe(Si*t*Bu3)2, Si*i*PrDis2, Tbt, and Ar* is studied using density functional theory (M06-2X/Def2-TZVP, B3PW91/Def2-TZVP and B3LYP/LANL2DZ + dp). The theoretical results demonstrate that all triply bonded RE13 ≡ PR compounds with small substituents are unstable and spontaneously rearrange to other doubly bonded isomers. That is, the smaller groups, such as R = F, OH, H, CH3 and SiH3, neither kinetically nor thermodynamically stabilize the triply bonded RE13 ≡ PR compounds. However, the triply bonded R′E13≡PR′ molecules, possessing bulkier substituents (R′ = SiMe(Si*t*Bu3)2, Si*i*PrDis2, Tbt and Ar*), are found to have a global minimum on the singlet potential energy surface. In particular, the bonding character of the R′E13≡PR′ species is well defined by the valence-electron bonding model (model [II]). That is to say, R′E13≡PR′ molecules that feature groups are regarded as R′-E13≡P-R′. The theoretical evidence shows that both the electronic and the steric effects of bulkier substituent groups play a prominent role in rendering triply bonded R′E13≡PR′ species synthetically accessible and isolable in a stable form.

**Keywords:** phosphorus, group 13 elements, triple bond, substituent effects, valence electrons

## 1. Introduction

Phosphorus is an interesting element, but many chemists have a poor comprehension of its bonding properties. Even though phosphorus and nitrogen belong to the same group in the periodic table, molecular nitrogen is a triply bonded diatomic molecule, but elemental white phosphorus is a tetrahedral compound wherein each atom is connected by three single bonds to the other atoms in the molecule. Phosphorus is usually connected to other elements by a

single chemical bond, which has been verified by lot of experimental evidences [1–14]. Also, molecules that feature a phosphorus double bond have been the subject of many experimental and theoretical studies of structure and reactivity [15–27]. However, little is known about the molecules that feature a phosphorus triple bond [28–32]. In particular, whether it is possible to anticipate the stability of the R-E13 $\equiv$ phosphorus-R (E13 = B, Al, Ga, In, and Tl) species based on the effects of substituents, since the R-E13 $\equiv$ phosphorus-R systems are isoelectronic to the R-E14 $\equiv$ E14-R (E14 = C, Si, Ge, Sn, and Pb) compound from the valence electron viewpoints.

This study uses the heavier acetylene analogue, R-E13 $\equiv$ P-R as a model molecule to determine the possibility of generating stable RE13PR species that feature the E13 $\equiv$ P triple bond. In order to understand the effects of substituents on the stability of triply bonded RE13 $\equiv$ PR molecules, both small and bulky groups are chosen in this work. A better understanding of the bonding character and the structure of triply bonded RE13 $\equiv$ PR species will allow experimental chemists to discover novel and stable molecules that feature the E13 $\equiv$ P triple bond.

## 1.1. General considerations

This section uses a simple valence-electron bonding model to demonstrate the bonding nature of substituted triply bonded RE13$\equiv$PR compounds.

First, the RE13$\equiv$PR species is separated into two units: R-E13 and R-P. **Figure 1** shows that these two fragments represent two types of valence-electron bonding model (model [I] and model [II]). Therefore, the R-E13 moiety and the R-P component have two and four valence electrons, respectively. The computational results show that the ground states of these two units are a singlet for R-E13 ([R-E13]$^1$) and a triplet for R-P ([R-P]$^3$). Therefore, model [I] in **Figure 1** is considered as [R-E13]$^1$ + [R-P]$^1$ $\rightarrow$ [R-E13$\equiv$P-R]$^1$ and model [II] is given as [R-E13]$^3$ + [R-P]$^3$ $\rightarrow$ [R-E13$\equiv$P-R]$^1$.

If the excitation energy ($\Delta E1$) from the triplet ground state to the singlet excited state for R-P is smaller than that for R-E13, then model [I] can be used to interpret the bonding character of RE13$\equiv$PR. That is, model [I] demonstrates that the triple bond in RE13$\equiv$PR is a single donor-acceptor (E13 $\rightarrow$ P) $\sigma$ bond and two donor-acceptor (E13 $\leftarrow$ P) $\pi$ bonds. Therefore, the bonding character of RE13$\equiv$PR can be viewed as RE13$\leqslant$PR. However, if the promotion energy ($\Delta E2$) from the singlet ground state to the triplet excited state for R-E13 is smaller than that for R-P, then model [II] can be used to explain the bonding character of RE13$\equiv$PR. Namely, model [II] shows that the triple bond in RE13 $\equiv$ PR is a single traditional $\sigma$ bond, a single traditional $\pi$ bond and a single donor-acceptor (E13 $\leftarrow$ P) $\pi$ bond, so its bonding character can be viewed as RE13$\leqslant$PR.

From model [I] and model [II] shown in **Figure 1**, two points need to be emphasized here. First, it is experimentally known that the covalent radius decreases as: Tl (148 pm) > In (142 pm) > Ga (122 pm) > Al (121 pm) > P(107 pm) > B (84 pm) [33]. Therefore, a large difference in the atomic radius results in a significant reduction in the overlap populations between E13 and phosphorus. Consequently, the bonding strength between phosphorus and the E13 element in the heteroatomic analogues of acetylene (RE13$\equiv$PR) should be weak. Second, the $\pi$ bond in the RE13 $\equiv$ PR species is also attributed to the lone pair of the R-P moiety, which is donated into the empty p-$\pi$ orbital of the R-E13 unit. Since the lone pair of the R-P component
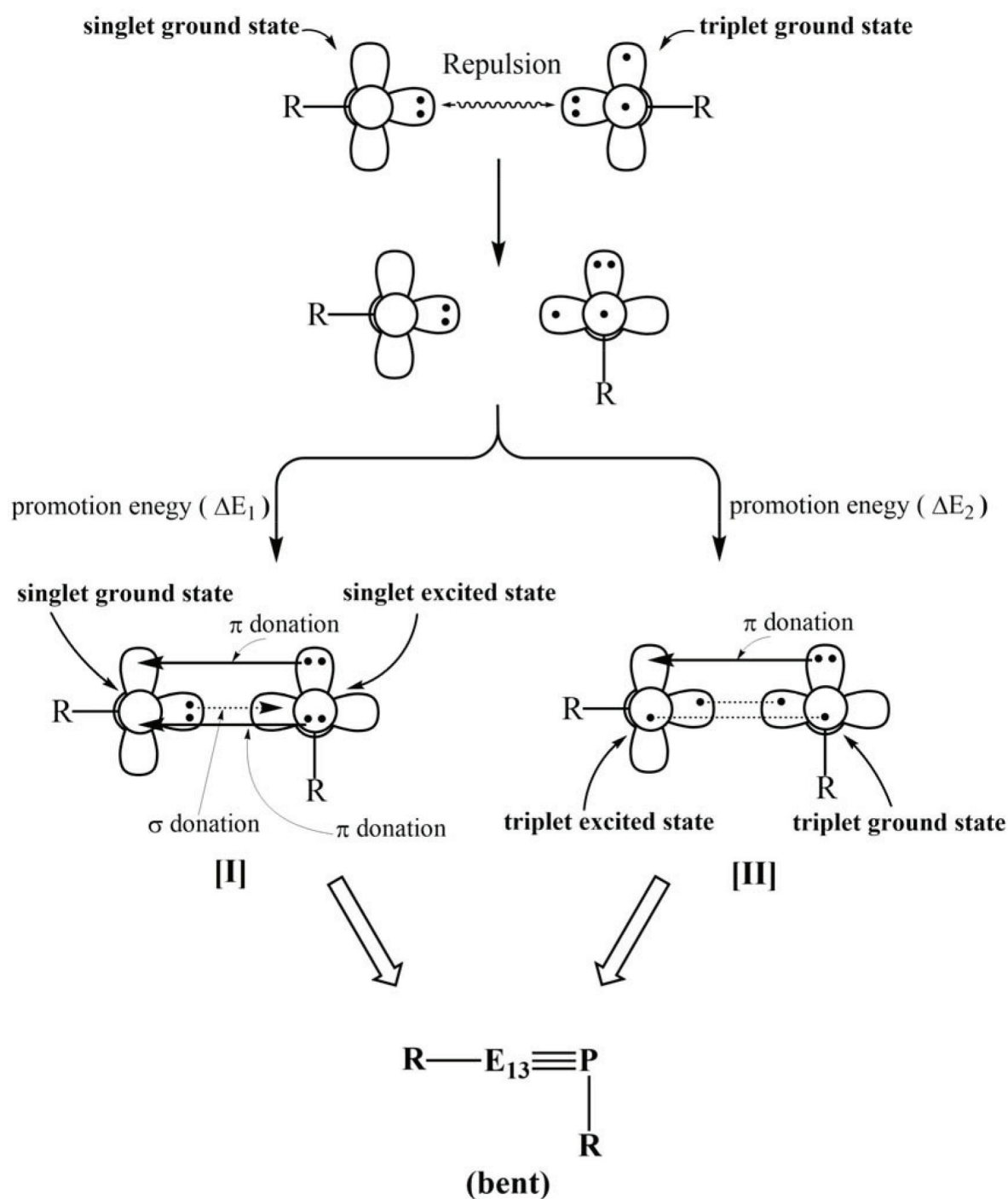
**Figure 1.** The valence-bond bonding models ([I] and [II]) for the triply bonded RE13 ≡ PR compound.

contains the s valence orbital of phosphorus and the p valence orbital of phosphorus is not the same size as that of the E13 atom, the overlap in the orbital populations between the P and E13 elements is small. In other words, on the basis of the bonding models that are shown in **Figure 1**, the triple bond between E13 and phosphorus is predicted to be very weak.

The computational evidences for these predictions are given in the following sections.

## 2. Results and discussion

### 2.1. Small ligands on substituted RE13 ≡ PR

Five small substituents (R), including F, OH, H, CH3 and SiH3, are initially chosen for this study. Three types of density functional theory (DFT) (M06-2X/Def2-TZVP, B3PW91/Def2-TZVP and B3LYP/LANL2DZ + dp) are used to determine the relative stability of the triply bonded RE13≡PR species and its corresponding doubly bonded isomers (R2E13 = P: and: E13 = PR2). In other words, two types of the 1,2-substituent-shift reactions (RE13≡PR → TS1 → R2E13 = P: and RE13≡PR → TS2 →: E13 = PR2) are studied. The respective computational results for RB≡PR [28], RAl≡PR [29], RGa≡PR [30], RIn≡PR [31], and RTl≡PR [32] are schematically shown in **Figures 2–6**.

The computational results that are shown in **Figures 2–6** show that regardless of the type of small substituent that is chosen, the triply bonded RE13 ≡ PR compound cannot be stabilized on the 1,2-migration energy surfaces. That is to say, it is easy for the RE13PR species to migrate to the corresponding doubly bonded R2E13 = P: or: E13 = PR2 isomers rather than to the triply bonded RE13 ≡ PR molecules. The theoretical evidence strongly suggests that the experimental detection of RE13≡PR that features small groups is very unlikely so they are not discussed in this section [28–32].

### 2.2. Large ligands on substituted R′E13 ≡ PR′

Four bulky groups (R′) are used to study the effects of substituents on the triply bonded RE13≡PR molecules. These are SiMe(Si*t*Bu3)2, Si*i*PrDis2, Tbt (C6H2–2,4,6-{CH(SiMe3)2}3) and Ar* (C6H3–2,6-(C6H2–2,4,6-*i*-Pr3)2) [34, 35]. In order to avoid the London dispersion forces [36], the dispersion-corrected M06-2X/Def2-TZVP level of theory [37] is used to compute geometrical parameters and some properties. The respective results for RB≡PR [28], RAl≡PR [29], RGa≡PR [30], RIn≡PR [31], and RTl≡PR [32] are shown in **Tables 1–5**. The same level of theory is also used to determine the feasibility of producing triply bonded R′E13 ≡ PR′ compounds (**Scheme 1** and **Tables 1–5**).

1. For bulky groups (R′), the E13≡P triple bond distances (Å) are anticipated to be in the range, 1.736–2.023 (B≡P), 2.152□2.183 (Al≡P), 2.146–2.183 (Ga≡P), 2.215–2.362 (In≡P) and 2.336–2.386 (Tl≡P).

2. The computed reaction enthalpies (ΔH1 and ΔH2) that are shown in **Scheme 1** and **Tables 1–5** show that regardless of the bulky ligand that is chosen, the energy of the triply bonded R′E13 ≡ PR′ species is much lower than those of its corresponding doubly bonded R′2E13 = P: or: E13 = PR′2 isomers. This computational evidence indicates that sterically congested ligands kinetically stabilize the triply bonded R′E13 ≡ PR′ compound.

3. The theoretical data in **Tables 1–5** show that the R′-E13 moiety has a singlet ground state, but the R′-P component has a triplet ground state. The production of the triply bonded

**Figure 2.** The relative Gibbs free energy surfaces for RB ≡ PR (R ═ H, F, OH, SiH3, and CH3). These energies are calculated in kcal/mol and are calculated at the M06-2X/Def2-TZVP, B3PW91/Def2-TZVP, and B3LYP/LANL2DZ + dp levels of theory.

**M06-2X/Def2-TZVP**
B3PW91/Def2-TZVP
B3LYP/LANL2DZ+dp
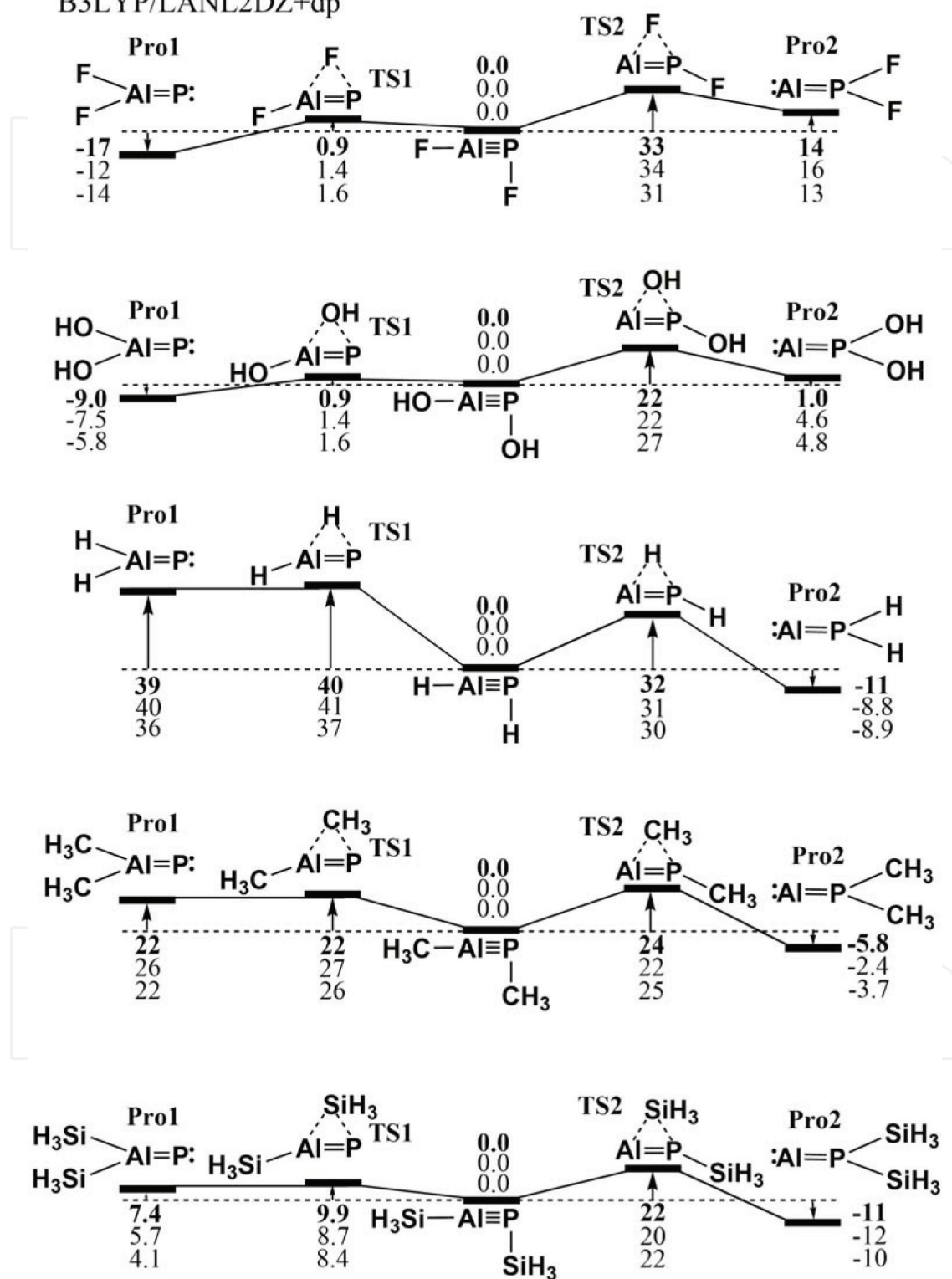


**Figure 3.** The relative Gibbs free energy surfaces for RAl ≡ PR (R ═ H, F, OH, SiH3, and CH3). These energies are calculated in kcal/mol and are calculated at the M06-2X/Def2-TZVP, B3PW91/Def2-TZVP, and B3LYP/LANL2DZ + dp levels of theory.
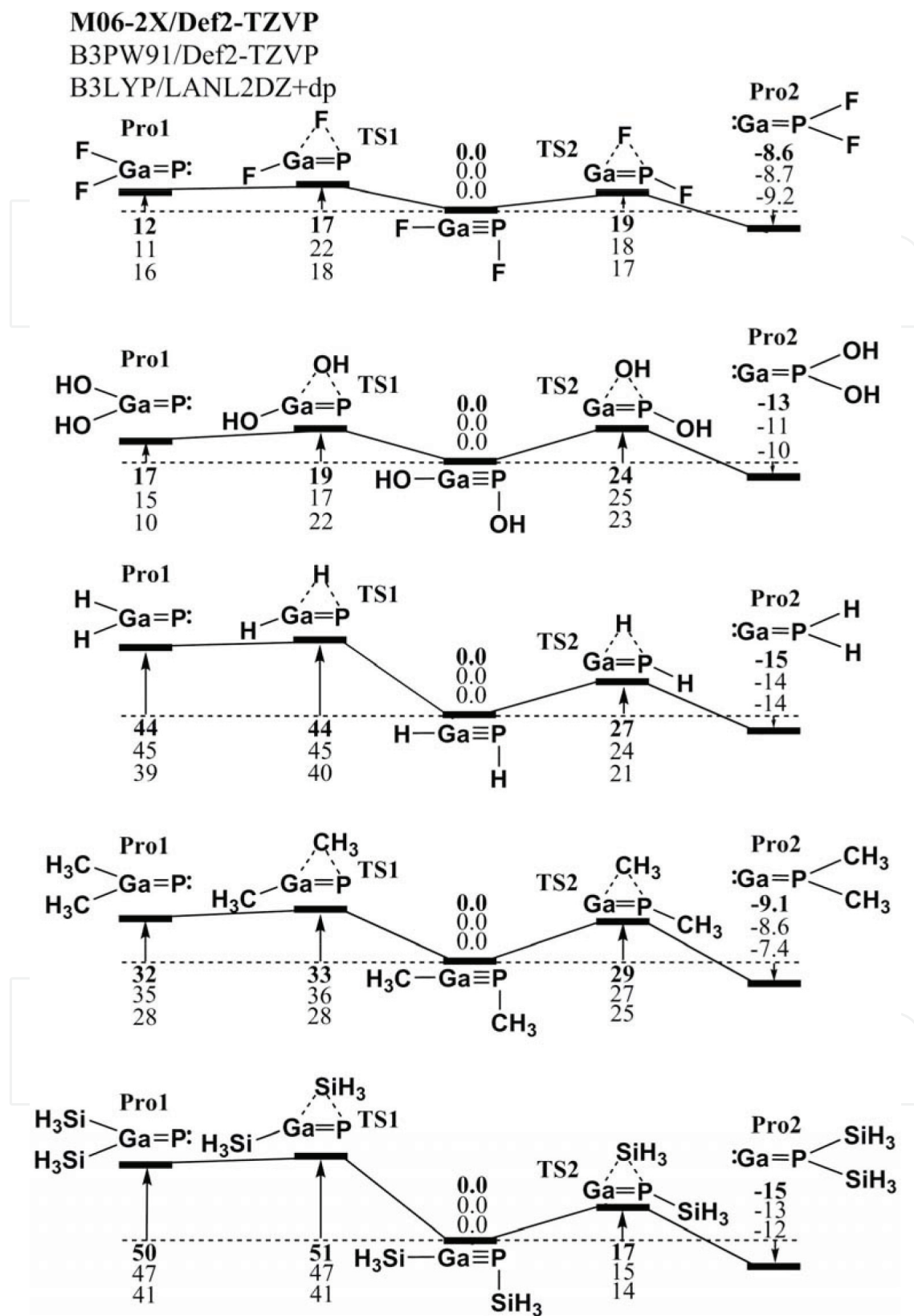
**Figure 4.** The relative Gibbs free energy surfaces for RGa ≡ PR (R ꞊ H, F, OH, SiH3, and CH3). These energies are calculated in kcal/mol and are calculated at the M06-2X/Def2-TZVP, B3PW91/Def2-TZVP, and B3LYP/LANL2DZ + dp levels of theory.

**Figure 5.** The relative Gibbs free energy surfaces for RIn ≡ PR (R = H, F, OH, SiH3, and CH3). These energies are calculated in kcal/mol and are calculated at the M06-2X/Def2-TZVP, B3PW91/Def2-TZVP, and B3LYP/LANL2DZ + dp levels of theory.
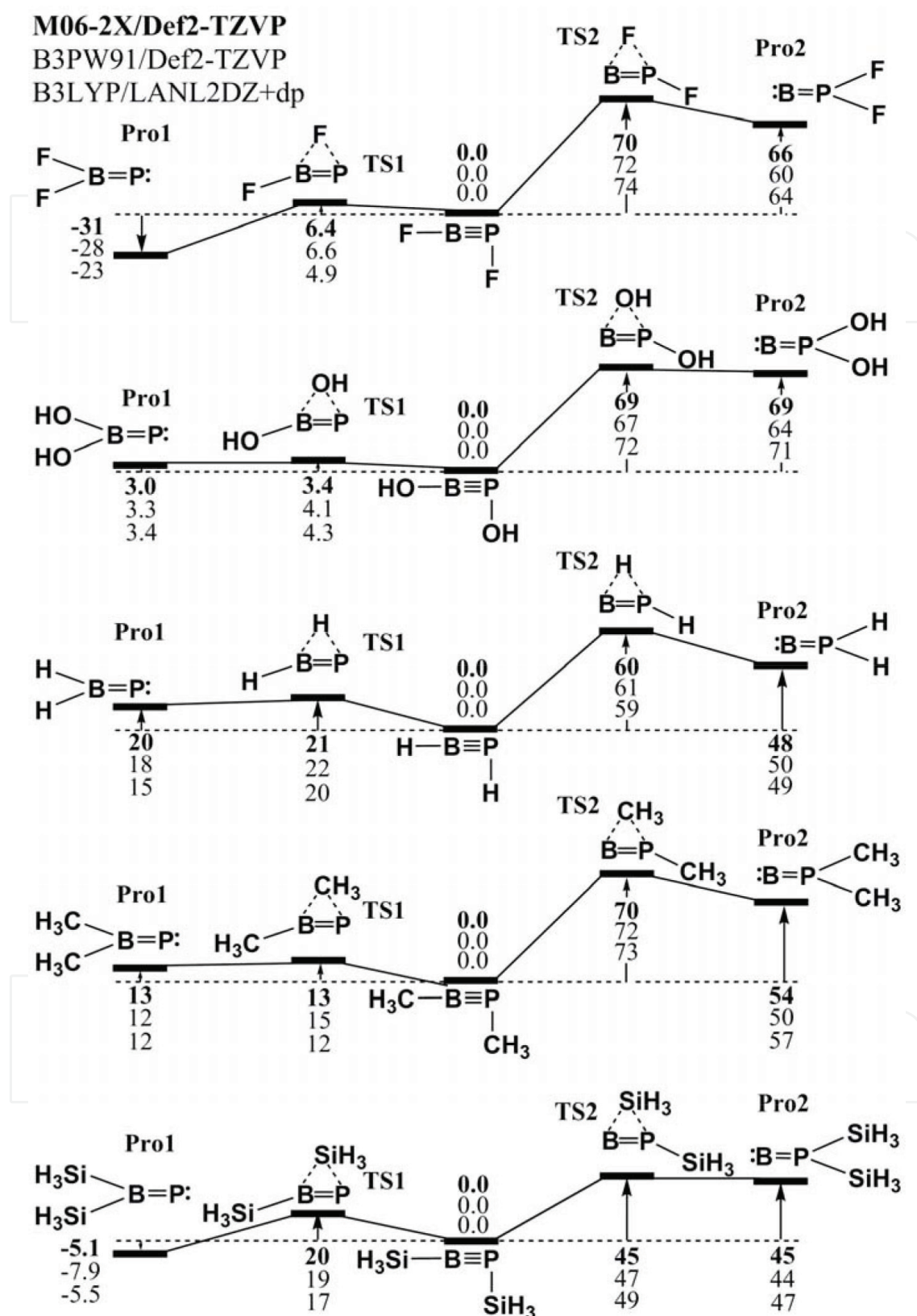
**Figure 6.** The relative Gibbs free energy surfaces for RTl ≡ PR (R = H, F, OH, SiH3, and CH3). These energies are calculated in kcal/mol and are calculated at the M06-2X/Def2-TZVP, B3PW91/Def2-TZVP, and B3LYP/LANL2DZ + dp levels of theory.

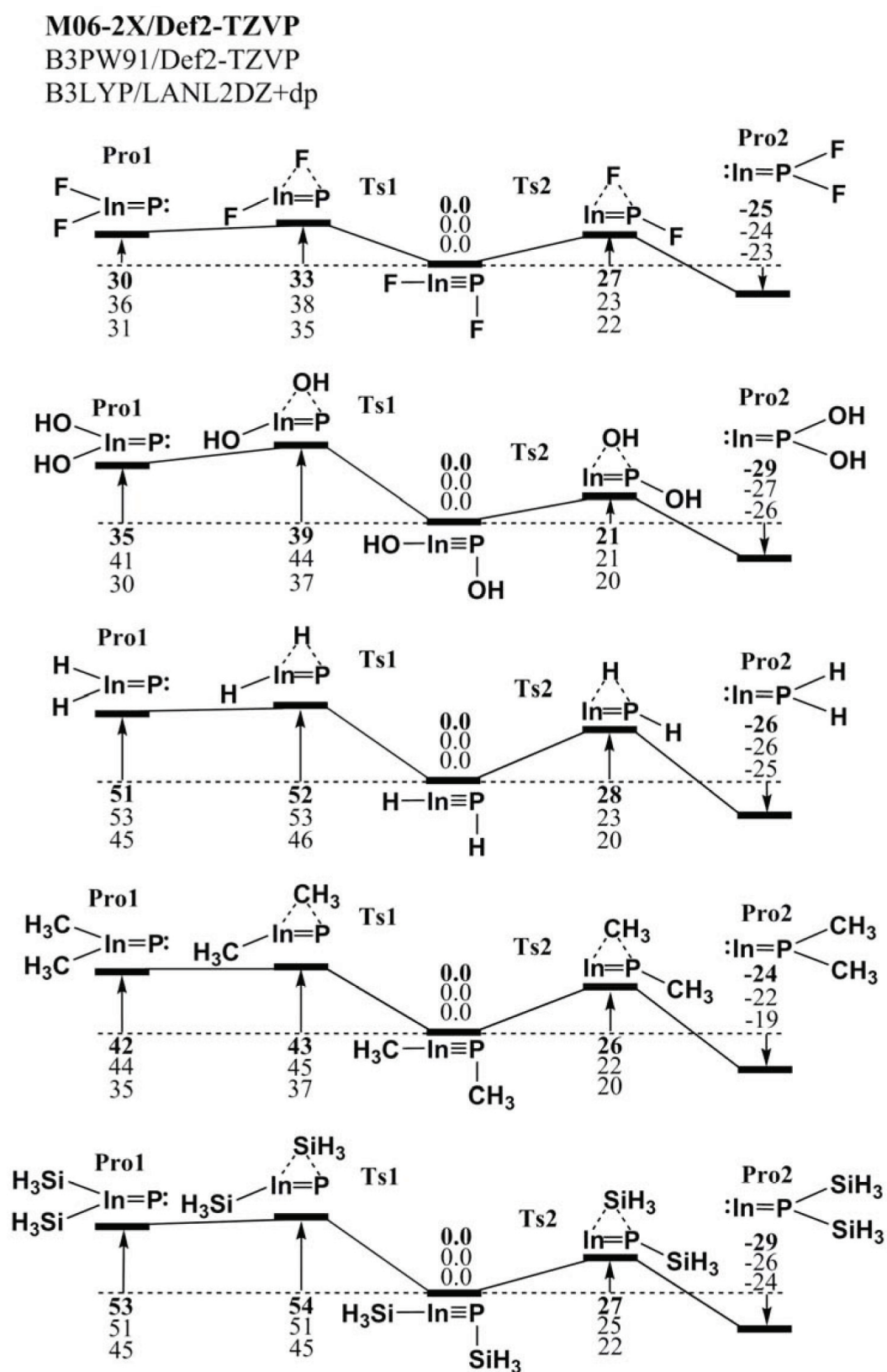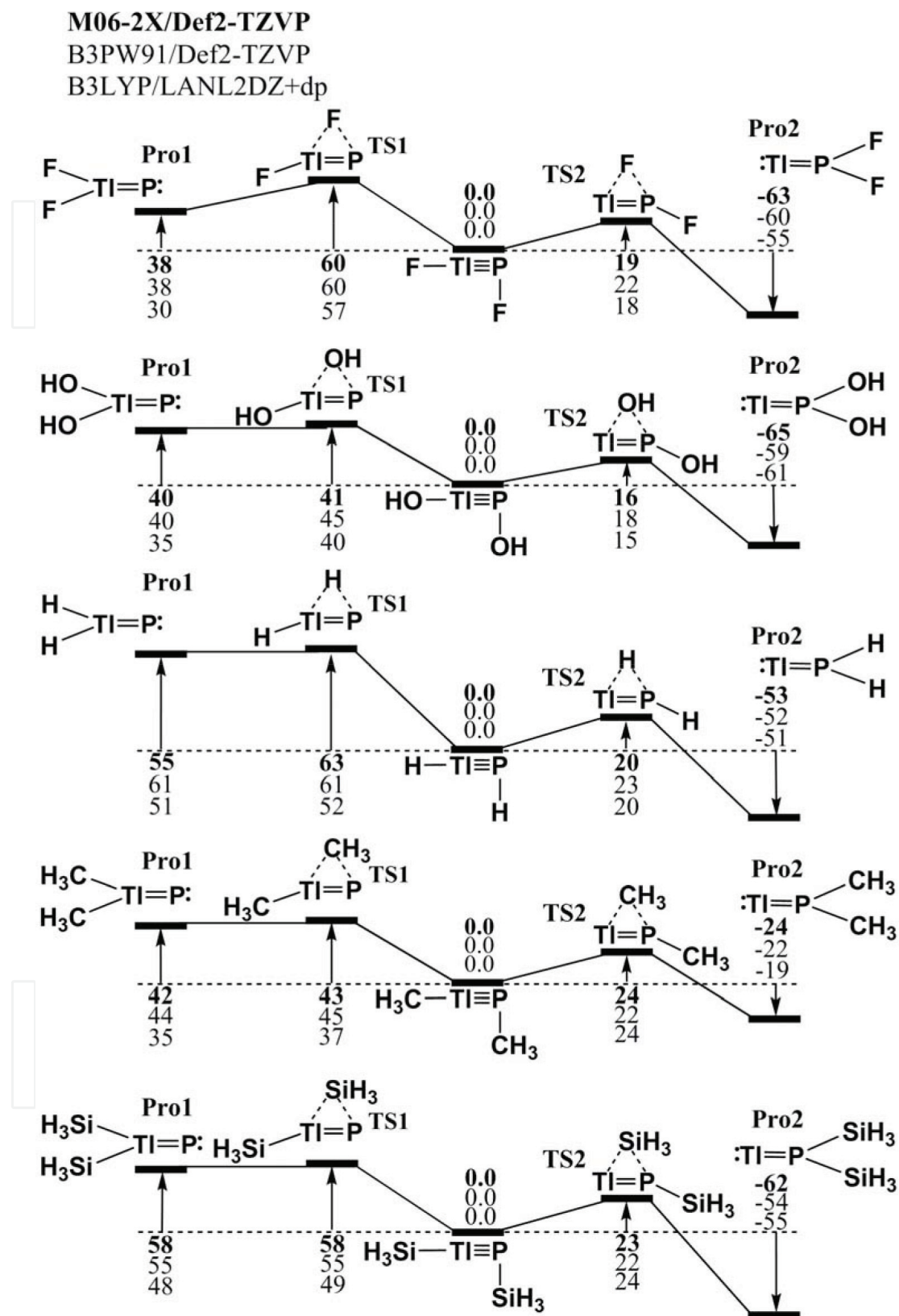R′E13 ≡ PR′ compound at the singlet ground state constitutes a combination of two triplet units, [R′-E13]$^3$ and [R′-P]$^3$. Therefore, using the information in **Figure 1**, the bonding nature of the E13 ≡ P triple bond in R′E13 ≡ PR′ can be regarded as RE13⪮PR.

4.   The theoretical analyses in Section II shows that the bond order for the E13 ≡ P triple bond should be very weak. **Tables 1–5** show that the Wiberg bond indices (WBI) [28, 39] for RE13≡PR compounds that feature sterically bulky substituents are all a little greater than 2.0. The theoretical evidence demonstrates that RE13≡PR that features bulky groups has only a weak triple bond because the WBI for the C≡C bond in acetylene is computed to be 2.99.

The results of this study show that successful schemes for the synthesis and isolation of triply bonded RE13≡PR molecules are imminent.

| R′ | SiMe(SitBu$_3$)$_2$ | SiiPrDis$_2$ | Tbt | Ar* |
|---|---|---|---|---|
| B ≡ P(Å) | 1.736 | 2.021 | 2.023 | 2.021 |
| ∠R′-B-P (°) | 157.2 | 166.0 | 164.4 | 166.6 |
| ∠B-P-R′ (°) | 122.0 | 112.5 | 121.3 | 123.3 |
| ∠R′-B-P-R′ (°) | 174.7 | 165.5 | 168.9 | 169.5 |
| Q$_B$′[1] | −0.2574 | −0.1395 | 0.2718 | 0.3520 |
| Q$_P$′[2] | −0.1824 | −0.3922 | 0.2260 | 0.2522 |
| ΔEB′ for R′-B (kcal/mol)[3] | 25.92 | 24.86 | 28.76 | 34.64 |
| ΔEP′ for R′-P (kcal/mol)[4] | −33.10 | −37.47 | −29.74 | −30.52 |
| HOMO-LUMO (kcal/mol) | 73.76 | 43.44 | 47.10 | 41.60 |
| BE (kcal/mol)[5] | 89.54 | 90.37 | 85.42 | 71.43 |
| ΔH$_1$ (kcal/mol)[6] | 73.75 | 86.65 | 87.89 | 87.59 |
| ΔH$_2$ (kcal/mol)[6] | 80.53 | 77.67 | 101.7 | 88.01 |
| WBI[7] | 2.388 | 2.152 | 1.963 | 1.966 |

[1]The natural charge density on the boron atom.
[2]The natural charge density on the phosphorus atom.
[3]ΔEB′ (kcal mol$^{-1}$) = E(triplet state for R′-B)–E(singlet state for R′-B).
[4]ΔEP′ (kcal mol$^{-1}$) = E(triplet state for R′-P)–E(singlet state for R′-P).
[5]BE (kcal mol$^{-1}$) = E(triplet state for R′-B) + E(triplet state for R′-P)–E(singlet for R′B ≡ PR′).
[6]See **Scheme 1**.
[7]The Wiberg bond index (WBI) for the B≡P bond: see references [38, 39].

**Table 1.** The bond lengths (Å), bond angles (°), singlet-triplet energy splitting (ΔEB′ and ΔEP′), natural charge densities (QB′ and QP′), binding energies (BE), the Wiberg bond index (WBI), HOMO-LUMO energy gaps, and some reaction enthalpies for R′B ≡ PR′ at the M06-2X/Def2-TZVP level of theory.

| R′ | SiMe(Si*t*Bu$_3$)$_2$ | Si*i*PrDis$_2$ | Tbt | Ar* |
|---|---|---|---|---|
| Al ≡ P(Å) | 2.168 | 2.152 | 2.183 | 2.175 |
| ∠R′-Al-P (°) | 166.5 | 163.4 | 165.0 | 167.3 |
| ∠Al-P-R′ (°) | 117.4 | 119.7 | 122.1 | 121.3 |
| ∠R′-Al-P-R′ (°) | 166.4 | 163.8 | 168.5 | 167.5 |
| Q$_{Al}$′[1] | 0.9712 | 0.9210 | 1.1072 | 1.326 |
| Q$_P$′[2] | −0.8751 | −0.9674 | −0.3430 | −0.359 |
| ΔEAl′ for Al-R′ (kcal/mol)[3] | 28.89 | 29.30 | 42.50 | 40.22 |
| ΔEP′ for P-R′ (kcal/mol)[4] | −23.10 | −27.47 | −30.51 | −28.52 |
| HOMO-LUMO (kcal/mol) | 52.74 | 34.83 | 49.98 | 57.15 |
| BE (kcal/mol)[5] | 43.49 | 54.96 | 47.51 | 35.41 |
| ΔH$_1$ (kcal/mol)[6] | 95.15 | 85.23 | 91.83 | 85.60 |
| ΔH$_2$ (kcal/mol)[6] | 96.13 | 82.75 | 90.56 | 85.31 |
| WBI[7] | 1.572 | 1.592 | 1.685 | 1.534 |

[1]The natural charge density on the aluminum atom.
[2]The natural charge density on the phosphorus atom.
[3]ΔEAl′ (kcal mol$^{-1}$) = E(triplet state for R′-Al)–E(singlet state for R′-Al).
[4]ΔEP′ (kcal mol$^{-1}$) = E(triplet state for R′-P)–E(singlet state for R′-P).
[5]BE (kcal mol$^{-1}$) = E(triplet state for R′-Al) + E(triplet state for R′-P)–E(singlet for R′Al≡PR′).
[6]See **Scheme 1**.
[7]The Wiberg bond index (WBI) for the Al≡P bond: see reference [38, 39].

**Table 2.** The bond lengths (Å), bond angles (°), natural charge densities (QAl′ and QP′), singlet-triplet energy splitting for Al-R′ and P-R′ units (ΔEAl′ and ΔEP′), binding energies (BE), HOMO-LUMO energy gaps, Wiberg bond index (WBI), and some reaction enthalpies for R′Al ≡ PR′ at the dispersion-corrected M06-2X/Def2-TZVP level of theory.

| R′ | SiMe(Si*t*Bu$_3$)$_2$ | Si*i*PrDis$_2$ | Tbt | Ar* |
|---|---|---|---|---|
| Ga ≡ P (Å) | 2.167 | 2.146 | 2.172 | 2.183 |
| ∠R′-Ga-P (°) | 158.2 | 161.3 | 152.0 | 158.4 |
| ∠Ga-P-R′ (°) | 127.8 | 120.4 | 117.3 | 126.1 |
| ∠R′-Ga-P-R′ (°) | 176.0 | 175.5 | 169.4 | 166.9 |
| Q$_{Ga}$′[1] | 0.8023 | 0.8266 | 0.8952 | 0.9003 |
| Q$_P$′[2] | −0.7655 | −0.7473 | −0.8662 | −0.8825 |
| ΔE$_{ST}$ for Ga-R′ (kcal/mol)[3] | 30.71 | 31.34 | 34.08 | 38.35 |
| ΔE$_{ST}$ for P-R′ (kcal/mol)[4] | −23.10 | −27.47 | −23.51 | −20.52 |
| HOMO-LUMO (kcal/mol) | 83.14 | 81.83 | 73.50 | 71.34 |
| BE (kcal/mol)[5] | 91.53 | 102.9 | 85.34 | 89.46 |
| ΔH$_1$ (kcal/mol)[6] | 89.11 | 94.82 | 86.31 | 98.94 |

| R′ | SiMe(Si*t*Bu₃)₂ | Si*i*PrDis₂ | Tbt | Ar* |
|---|---|---|---|---|
| $\Delta H_2$ (kcal/mol)[6] | 86.43 | 85.91 | 88.53 | 84.08 |
| WBI[7] | 2.228 | 2.235 | 2.017 | 2.114 |

[1]The natural charge density on the gallium atom.
[2]The natural charge density on the phosphorus atom.
[3]$\Delta E_{ST}$ (kcal mol$^{-1}$) = E(triplet state for R′-Ga)–E(singlet state for R′-Ga).
[4]$\Delta E_{ST}$ (kcal mol$^{-1}$) = E(triplet state for R′-P)–E(singlet state for R′-P).
[5]BE (kcal mol$^{-1}$) = E(triplet state for R′-Ga) + E(triplet state for R′-Ga)–E(singlet for R′Ga $\equiv$ PR′).
[6]See **Scheme 1**.
[7]The Wiberg bond index (WBI) for the Ga$\equiv$P bond: see reference [38, 39].

**Table 3.** The bond lengths (Å), bond angles (°), natural charge densities (QGa′ and QP′), singlet-triplet energy splitting ($\Delta E$ST), binding energies (BE), the HOMO-LUMO energy gaps, the Wiberg bond index (WBI), and some reaction enthalpies for R′Ga $\equiv$ PR′ at the dispersion-corrected M06-2X/Def2-TZVP level of theory.

| R′ | SiMe(Si*t*Bu₃)₂ | Si*i*PrDis₂ | Tbt | Ar* |
|---|---|---|---|---|
| In$\alpha$P(Å) | 2.362 | 2.337 | 2.215 | 2.238 |
| ∠R′-In-P (°) | 169.6 | 175.0 | 177.9 | 171.4 |
| ∠In-P-R′ (°) | 115.0 | 112.0 | 113.2 | 115.1 |
| ∠R′-In-P-R′ (°) | 177.5 | 172.47 | 175.4 | 172.3 |
| $Q_{In}$′[1] | 1.1046 | 0.9396 | 0.9489 | 0.9553 |
| $Q_P$′[2] | −0.9546 | −0.9363 | −0.8560 | −0.6715 |
| $\Delta E_{ST}$ for In-R′ (kcal/mol)[3] | 33.93 | 29.53 | 22.48 | 28.41 |
| $\Delta E_{ST}$ for P-R′ (kcal/mol)[4] | −28.51 | −27.58 | −25.64 | −22.31 |
| HOMO-LUMO (kcal/mol) | 74.96 | 72.41 | 87.56 | 88.43 |
| BE (kcal/mol)[5] | 86.51 | 84.30 | 92.61 | 90.64 |
| $\Delta H_1$ (kcal/mol)[6] | 92.07 | 90.08 | 97.41 | 87.46 |
| $\Delta H_2$ (kcal/mol)[6] | 88.35 | 89.18 | 89.26 | 79.32 |
| WBI[7] | 2.263 | 2.251 | 2.188 | 2.174 |

[1]The natural charge density on the central indium atom.
[2]The natural charge density on the central phosphorus atom.
[3]$\Delta E_{ST}$ (kcal mol$^{-1}$) = E(triplet state for R′-In)–E(singlet state for R′-In).
[4]$\Delta E_{ST}$ (kcal mol$^{-1}$) = E(triplet state for R′-P)–E(singlet state for R′-P).
[5]BE (kcal mol$^{-1}$) = E(triplet state for R′-In) + E(triplet state for R′-P)–E(singlet for R′In $\equiv$ PR′).
[6]See **Scheme 1**.
[7]The Wiberg bond index (WBI) for the In$\equiv$P bond: see reference [38, 39].

**Table 4.** The bond lengths (Å), bond angles (°), singlet-triplet energy splitting ($\Delta E$ST), natural charge densities (QIn′ and QP′), binding energies (BE), the HOMO-LUMO energy gaps, the Wiberg bond index (WBI), and some reaction enthalpies for R′In$\equiv$PR′ at the B97-D3/LANL2DZ + dp level of theory.

| R′ | SiMe(Si$t$Bu$_3$)$_2$ | Si$i$PrDis$_2$ | Tbt | Ar* |
|---|---|---|---|---|
| Tl ≡ P(Å) | 2.386 | 2.384 | 2.385 | 2.336 |
| ∠R′–Tl-P (°) | 166.9 | 166.4 | 168.9 | 161.2 |
| ∠Tl–P–R′ (°) | 122.3 | 113.7 | 116.2 | 115.6 |
| ∠R′–Tl–P–R′ (°) | 171.4 | 179.5 | 173.9 | 174.4 |
| $Q_{Tl}'$[1] | 0.975 | 0.739 | 1.166 | 1.218 |
| $Q_P'$[2] | −0.860 | −0.826 | −0.344 | −0.257 |
| $\Delta E_{ST}$ for Tl–R′ (kcal/mol)[3] | 35.91 | 35.52 | 31.27 | 30.24 |
| $\Delta E_{ST}$ for P–R′ (kcal/mol)[4] | −43.10 | −37.47 | −39.74 | −40.52 |
| HOMO-LUMO (kcal/mol) | 71.27 | 27.21 | 58.05 | 39.34 |
| BE (kcal/mol)[5] | 80.24 | 85.43 | 62.51 | 67.89 |
| $\Delta H_1$ (kcal/mol)[6] | 91.34 | 90.49 | 89.22 | 87.11 |
| $\Delta H_2$ (kcal/mol)[6] | 73.98 | 72.83 | 71.27 | 74.01 |
| WBI[7] | 2.116 | 2.273 | 2.127 | 2.201 |

[1]The natural charge density on the central thallium atom.
[2]The natural charge density on the central phosphorus atom.
[3]$\Delta E_{ST}$ (kcal mol$^{-1}$) = E(triplet state for R′-Tl)–E(singlet state for R′-Tl).
[4]$\Delta E_{ST}$ (kcal mol$^{-1}$) = E(triplet state for R′-P)–E(singlet state for R′-P).
[5]BE (kcal mol$^{-1}$) = E(triplet state for R′-Tl) + E(singlet state for R′-P)–E(singlet for R′Tl ≡ PR′).
[6]See **Scheme 1**.
[7]The Wiberg bond index (WBI) for the Tl≡P bond: see reference [38, 39].

**Table 5.** The bond lengths (Å), bond angles (°), singlet-triplet energy splitting ($\Delta E$ST), natural charge densities ($Q_{Tl}'$ and $Q_P'$), binding energies (BE), the HOMO-LUMO energy gaps, the Wiberg bond index (WBI), and some reaction enthalpies for R′Tl ≡ PR′ at the dispersion-corrected M06-2X/Def2-TZVP level of theory.



(R′ = SiMe(Si$t$Bu$_3$)$_2$, Si$i$PrDis$_2$, Tbt, and Ar*)
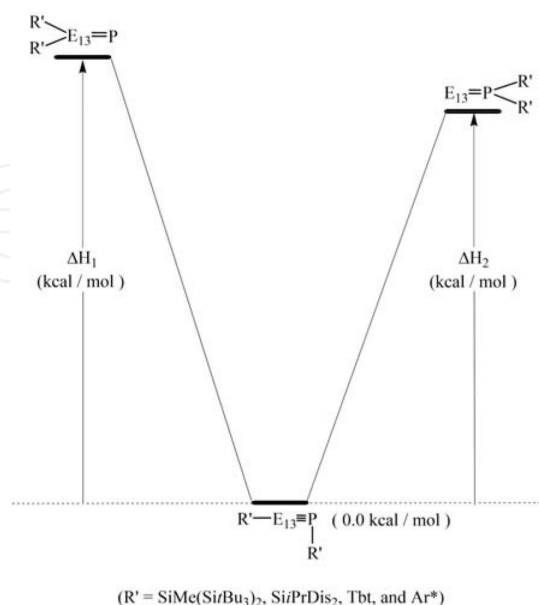
**Scheme 1.** Several important conclusions can be drawn from the results in **Tables 1–5**.

## Acknowledgements

## Author details

Jia-Syun Lu[1], Ming-Chung Yang[1] and Ming-Der Su[1,2]*

*Address all correspondence to: midesu@mail.ncyu.edu.tw

1  Department of Applied Chemistry, National Chiayi University, Chiayi, Taiwan

2  Department of Medicinal and Applied Chemistry, Kaohsiung Medical University, Kaohsiung, Taiwan

## References

[1] Nyhlen J, Privalov T. "Frustration" of orbital interactions in Lewis base/Lewis acid adducts: A computational study of $H_2$ uptake by phosphanylboranes $R_2P=BR'_2$. European Journal of Inorganic Chemistry. 2009;**15**:2759-2764

[2] Karsch HH, Hanika G, Huber B, Meindl K, Koöig S, Krüger C, Müller G. Monomeric phosphinoboranes: The role of the B- and P-substituents for P=B multiple bonding. Journal of the Chemical Society, Chemical Communications. 1989;**29**:373-375

[3] Kubo K, Kawanaka T, Tomioka M, Mizuta T. Synthesis and crystal structures of p-iron-substituted phosphinoborane monomers. Organometallics. 2012;**31**:2026-2034

[4] Allen TL, Scheiner AC, Schaefer HF III. Theoretical studies of borylphosphine, its conjugate base, and the lithium salt of its conjugate base. The use of orbital kinetic energies to determine the origin of the driving force for changes in molecular geometry. Inorganic Chemistry. 1990;**29**:1930-1936

[5] Gilbert TM, Bachrach SM. Computational studies of [2+2] and [4+2] pericyclic reactions between phosphinoboranes and alkenes. Steric and electronic effects in identifying a reactive phosphinoborane that should avoid dimerization. Organometallics. 2007;**26**:2672-2678

[6] Privalov T. On the possibility of conversion of alcohols to ketones and aldehydes by phosphinoboranes $R_2PBR'R''$: A computational study. Chemistry-A European Journal. 2009;**15**:1825-1829

[7] Kenward AL, Pierd WE. Heterolytic $H_2$ activation by nonmetals. Angewandte Chemie International Edition. 2008;**47**:38-41

[8] Coolidge MB, Borden WT. Ab initio calculations on borylphosphines: Prediction of a synergistic substituent effect in diborylphosphine. Journal of the American Chemical Society. 1990;**112**:1704-1706

[9] Geier SJ, Gilbert TM, Stephan DW. Activation of $H_2$ by phosphinoboranes $R_2PB(C_6F_5)_2$. Journal of the American Chemical Society. 2008;**130**:12632-12633

[10] Paetzold P. The p-centered chemistry of [(di-tert-butylphosphanyl)imino]-(2,2,6,6-tetramethylpiperidino)borane. Advances in Inorganic Chemistry. 1987;**31**:123-170

[11] Grant DJ, Dixon DA. Thermodynamic properties of molecular borane phosphines, alane amines, and phosphine alanes and the $[BH_4^-][PH_4^+]$, $[AlH_4^-][NH_4^+]$, and $[AlH_4^-][PH_4^+]$ salts for chemical hydrogen storage systems from ab initio electronic structure theory. The Journal of Physical Chemistry A. 2005;**109**:10138-10147

[12] Grant DJ, Dixon DA. $\sigma$- and $\pi$-bond strengths in main group 3−5 compounds. The Journal of Physical Chemistry A. 2006;**110**:12955-12962

[13] Ditty MJT, Power WP. $^{31}P$ chemical shielding as a function of bond angle: Phosphorus chemical shielding surface of phosphinoborane $R_2PBR'_2$. Canadian Journal of Chemistryan. 1999;**77**:1951-1961

[14] Jemmis ED, Subramanian G. Torsional barriers in $H_2B:XCH_3$ (X = NH, O, PH, and S). The Journal of Physical Chemistry. 1994;**98**:8937-8939

[15] Allen TL, Fink WH. Theoretical studies of borylphosphine and its conjugate base. 2. Internal rotation and inversion transition states. Inorganic Chemistry. 1992;**31**:1703-1705

[16] Magnusson E. Conformational energies and structural relaxation in singly bonded silicon, phosphorus and sulfur-compounds. Australian Journal of Chemistry. 1986;**39**:735-745

[17] Geier SJ, Gilbert TM, Stephan DW. Synthesis and reactivity of the phosphinoboranes $R_2PB$ $(C_6F_5)_2$. Inorganic Chemistry. 2011;**50**:336-344

[18] Stephan DW, Erker G. Frustrated Lewis pairs: Metal-free hydrogen activation and more. Angewandte Chemie International Edition. 2010;**49**:46-76

[19] Schulz S. Group 13/15 organometallic compounds-synthesis, structure, reactivity and potential applications. Advances in Organometallic Chemistry. 2003;**49**:225-439

[20] Pons V, Baker T. Soluble boron-nitrogen high polymers from metal-complex-catalyzed amine borane dehydrogenation. Angewandte Chemie International Edition. 2008;**47**:9600-9602

[21] Clark TJ, Lee K, Manners I. Transition-metal-catalyzed dehydrocoupling: A convenient route to bonds between main-group elements. Chemistry-A European Journal. 2006;**12**:8634-8648

[22] Jaska CA, Bartole-Scott A, Manners I. Metal-catalyzed routes to rings, chains and macromolecules based on inorganic elements. Dalton Transactions. 2003;**21**:4015-4021

[23] Maya L. Boron nitride precursors—A perspective. Applied Organometallic Chemistry. 1996;**10**:175-182

[24] Manners I. Polymers and the periodic table: Recent developments in inorganic polymer science. Angewandte Chemie International Edition in English. 1996;**35**:1602-1621

[25] Whittell GR, Manners I. Synthesis of ammonia borane nanoparticles and the diammoniate of diborane by direct combination of diborane and ammonia. Angewandte Chemie International Edition. 2011;**50**:10288-10289

[26] Hugle T, Hartl M, Lentz D. The route to a feasible hydrogen-storage material: MOFs versus ammonia borane. Chemistry-A European Journal. 2011;**17**:10184-10207

[27] Price AN, Nichol GS, Cowley MJ. Phosphaborenes: Accessible reagents for the synthesis of C-C/P-B isosteres. Angewandte Chemie International Edition. 2017;**56**:9953-9957

[28] Lu J-S, Yang M-C, Su M-D. Triple-bonded boron≡phosphorus molecule: Is that possible? ACS Omega. 2018;**3**:76-85

[29] Lu J-S, Yang M-C, Su M-D. Aluminum-phosphorus triple bonds: Do substituents make Al≡P synthetically accessible? Chemical Physics Letters. 2017;**686**:60-67

[30] Lu J-S, Yang M-C, Su M-D. Triply bonded gallium≡phosphorus molecules: Theoretical designs and characterization. The Journal of Physical Chemistry A. 2017;**121**:6630-6637

[31] Lu J-S, Yang M-C, Su M-D. Triply-bonded indium≡phosphorus molecules: Theoretical designs and characterization. American Chemical Society Omega. 2017;**2**:2813-2826

[32] Lu J-S, Yang M-C, Su M-D. Substituent effects on the stability of thallium and phosphorus triple bonds: A density functional study. Molecules. 2017;**22**:1111-1124

[33] Cordero B, Gómez V, Platero-Prats AE, Revés M, Echeverría J, Cremades E, Barragán F, Alvarez S. Covalent radii revisited. Dalton Transactions. 2008;(21):2832-2838

[34] Kobayashi K, Takagi N, Nagase S. Do bulky aryl groups make stable silicon-silicon triple bonds synthetically accessible? Organometallics. 2001;**20**:234-232

[35] Takagi N, Nagase S. Substituent effects on germanium-germanium and tin-tin triple bonds. Organometallics. 2001;**20**:5498-5500

[36] Liptrot DJ, Power PP. London dispersion forces in sterically crowded inorganic and organometallic molecules. Nature Reviews Chemistry. 2017;**1**:4

[37] Zhao Y, Truhlar DG. Density functionals with broad applicability in chemistry. Accounts of Chemical Research. 2008;**41**:157-167

[38] Wiberg KB. Application of the Pople-Santry-Segal CNDO method to the Cyclopropyl-carbinyl and Cyclobutyl cation and to Bicyclobutane. Tetrahedron. 1968;**24**:1083-1096

[39] Reed AE, Curtiss LA, Weinhold F. Intermolecular interactions from a natural bond orbital. Donor-Acceptor Viewpoint. Chemical Reviews. 1998;**88**:899-926